7.3.6 HET GCR trigger

In fig. 7.26 a sample trajectory for the GCR trigger is given. In this example the particle penetrates the outer segments of the B detectors and thus also penetrates the scintillation detector. The energy deposition in the scintillator is then added to a histogram.

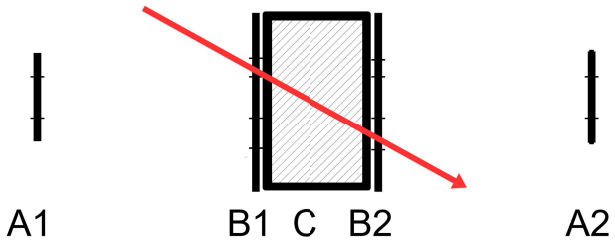


Figure 7.26: Example illustration of a valid GCR particle detection. The detection would also be valid for the inner segments of the B detectors.

The HET level 3 GCR trigger is an addition to the HET level 3 penetrating trigger which is described in sec. 7.3.5. The aim of the GCR trigger is to measure the rare GCR protons with the highest achievable field of view that HET can provide. The increase in the field of view is achieved by using only the two B detectors and the C detector. With this setting, not only particles entering the sensor head through the telescope opening are accepted, but also particles entering through the thin aluminum housing of the sensor head, so that the increase in field of view is on the cost of energy resolution. There are three entry points points to the HET level 3 GCR trigger. All particles, that are assigned trigger class 3 (see table 7.2) are tested at the beginning of the penetrating level 3 trigger regarding their coincidence conditions. If only a BB-coincidence is detected, the particle is directly sent to the GCR trigger. In case that an ABB-coincidence is detected, the particle is first evaluated by the penetrating trigger and afterwards sent to the GCR trigger, regardless of successful or unsuccessful evaluation by the penetrating level 3 trigger. The GCR trigger design is very similar to that of the HET penetrating trigger but highly reduced in complexity and thus reduced in code length and evaluation time.
The GCR trigger is explained using the flowchart in fig. 7.27. The first step, #1 in fig. 7.27, is that calibration factors are applied to the SSDs and the segment with the maximum energy deposition of each SSD is determined.
The next step, #2 in fig. 7.27, does the same for the scintillator C.
In the next step, #3 in fig. 7.27, B_{min} = min(B1,B2) is calculated for the further evaluation. Additionally, the highest measured signal in the anti-coincidence segments of the B detectors is defined as B3max = max(B1G,B2G).

Subsequently in the next step, #4 in fig. 7.27, the two values are compared. The maximum energy deposition in the anti-coincidence segments, B3max, is checked to be below 10% of B_{min}.

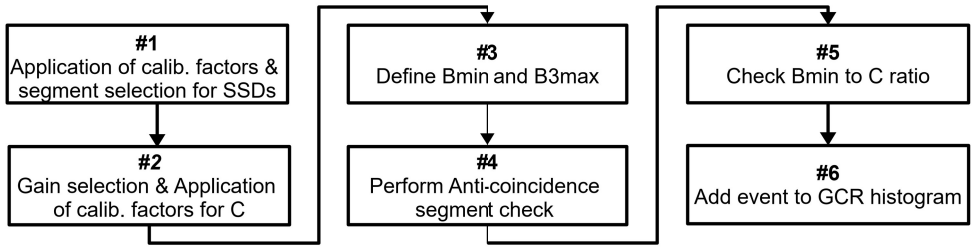


Figure 7.27: HET level 3 GCR trigger illustration using a flow chart. Each step is described in detail in the text.

Finally, the last evaluation step, #5 in fig. 7.27 is a comparison between Bmin and C, identical to the check performed in the penetrating trigger in #6 of fig. 7.21, to detect ion fragmentation.
If these evaluation steps are successful, as per step #6 in fig. 7.27, the particle is added to a 1D histogram of the energy deposition in C. The histogram is binned in 256 logarithmic bins with 16 bins per octave starting at 4 MeV up to 257 GeV. In fig. 7.28 the 1D GCR histogram for a proton simulation with a power law energy spectrum with an index of -1 ranging from 80 MeV to 2 GeV is given for illustration. The nominal data products cover an energy range for protons from 157 MeV up to relativistic energies (minimum ionizing particles).

7.3.7 High flux / nominal mode

Similar to the Electron Proton and Helium Instrument (EPHIN) on the SOlar Heliospheric Observatory (SOHO), HET features a special configuration for periods with high particle fluxes (Müller-Mellin et al., 1995). High particle fluxes may occur close to the Sun during intensive SEP events. During time periods with high particle fluxes, the HET data processing electronics may be saturated for the particle processing. This saturation may lead to dead time effects, so that not all events can be evaluated and even the chance of multi-coincidence detection of particles may occur. The latter case refers to the possibility, that two incoming primary particles can be detected as one single particle. To assure a full functionality of the instrument during these periods, the geometrical factor of HET can be reduced by a factor of ≈4.6. The reduction in geometrical factor is achieved, by increasing the level 1 threshold of the A outer segments. The geometrical factors for all trigger level 3 classes are calculated and given

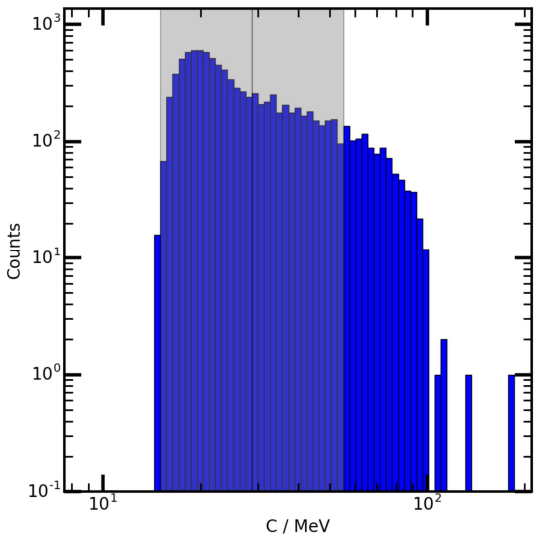


Figure 7.28: The 1D GCR histogram for a simulation of 80 MeV to 2 GeV protons. The visible peak in the histogram results from the relativistic proton which are MIPs. At higher deposited energies, where no data product items (black boxes) are placed, the proton population is contaminated by relativistic He ions, which are not shown here.

in sec. 9.2. The threshold is selected to suppress the particle species with the highest expected fluxes. These particles are electrons and protons in the ABnC energy range, as SEP event fluxes are reduced towards higher energies as shown in Mewaldt et al. (2005) for several ion species and electrons in different SEP events. An increase of the level 1 threshold of the A outer segments influences the ABC and penetrating level 3 trigger as well. The energy deposition of particles in the ABC and penetrating energy ranges in A is lower compared to particles in the ABnC level 3 trigger energy range. The effect of the increased threshold for all affected triggers is illustrated in fig. 7.29. The GCR trigger is unaffected by this threshold increase. The left panel (a) in fig. 7.29 shows the energy deposition in A plotted versus the summed up energy deposition in the A and B detectors (ABnC trigger). The black line illustrates the selected threshold of 6.2 MeV for the outer A detector segment in order to suppress the protons and electrons. Since higher energetic particles deposit less energy in the A detector according to the Bethe-Bloch equation (see eq. 3.1 in sec. 3.1), even heavier ion species than electrons and protons are suppressed in the ABC stopping and the penetrating trigger. This is illustrated by the black line in panels (b) and (c) in fig. 7.29. In case of the ABC stopping trigger, most of the ^{3}He and ^{4}He ion population is suppressed due to the threshold. In case of the penetrating trigger, ion species up to the CNO group are suppressed. For the affected ion species, the suppres-